Diamond & Related Materials 149 (2024) 111616

Contents lists available at ScienceDirect

Diamond & Related Materials

journal homepage: www.elsevier.com/locate/diamond

Nb-doped hydrogenated diamond-like carbon coated biodiesel injectors material: Synthesis, structure and properties

Ihsan Efeoglu [a], Md Abdul Maleque [b,*], Gokhan Gulten [a], Mustafa Yesilyurt [a], Banu Yaylali [a], Yasar Totik [a], Md Abul Kalam [c,*], Masjuki Haji Hassan [d], Nurin Wahidah Zulkifli [e]

[a] *Faculty of Engineering, Department of Mechanical Engineering, Atatürk University, 25240 Erzurum, Türkiye*
[b] *Department of Manufacturing & Materials Engineering, International Islamic University Malaysia, 53100 Kuala Lumpur, Malaysia*
[c] *School of Civil and Environmental Engineering, University of Technology Sydney, NSW 2007, Australia*
[d] *Department of Mechanical & Aerospace Engineering, International Islamic University Malaysia, Jalan Gombak 53100, Malaysia*
[e] *Department of Mechanical Engineering, University of Malaya, 50603 Kuala Lumpur, Malaysia*

A R T I C L E I N F O

Keywords:
Biodiesel engine injector materials
Nb-DLC coating
Closed field unbalanced magnetron sputtering
Structure
And property

A B S T R A C T

Despite the economic and environmental benefits of biodiesel, it poses significant challenges, including coking on metal surface and increased wear on diesel engine injector nozzles. Therefore, this study investigates the synthesis of niobium-doped diamond-like carbon (Nb-DLC) coatings on two types of injector nozzle materials (viz. H13 steel, AISI 420 stainless steel) using the Closed-Field Unbalanced Magnetron Sputtering (CFUBMS) technique. Comprehensive characterizations, including microstructural analysis, crystal structure evaluation, hardness assessment, and tribological property assessment, were conducted. The Nb-DLC coatings demonstrated a stable friction coefficient, with values four times lower than that of the substrate materials. The present findings demonstrate significant enhancements in terms of structural composition, crystalline phase, hardness, friction coefficients, and adhesion properties due to the Nb-DLC coatings. Therefore, Nb-DLC coated materials could be the promising candidate material for biodiesel engine injector nozzle applications. This emphasizes their potential to contribute significantly to the sustainable consolidation of biodiesel within automotive engine.

1. Introduction

At the beginning of this century, energy consumption and environmental sustainability became two of the most critical issues in the global community. The limited reserves of fossil fuels and the harmful environmental impacts caused by using these fuels brought about the need to explore alternative energy sources. In the quest for sustainable energy solutions, biodiesel has appeared as a favourable alternative derived from renewable sources of vegetable oils and animal fats. Biodiesel offers economic and environmental advantages with the potential to reduce carbon footprint, increase energy security and support economic development [1]. Therefore, biodiesel use is growing in the context of solving the global energy crisis and investing in a greener future [2]. However, there are some disadvantages to using biodiesel instead of traditional fossil fuels. These are; i) high viscosity, ii) low energy value, iii) higher nitrogen oxide (NOx) emissions, iv) lower engine speed and power, v) coking on injector nozzle metal surface (decarburization), and vi) higher injector surface wear [3–5].

The current state of injector nozzle materials, exposed to the challenges posed by biodiesel, is marked by premature failure and a limited operational lifespan. The wear properties of these materials require enhancement to mitigate premature failure, extending the working life of bio-diesel engine injector nozzle systems in the automotive sector. Moreover, the combustion chamber environment, characterized by high temperatures during fuel injection and combustion processes, impairs surface-related challenges for injector nozzle materials. With this regards, the issues of wear, friction, and the formation of coking on the injector nozzle surface pose difficulties that require a comprehensive solution. The lack of sustainable coating solutions such as DLC coating that can be designed for injector materials in the context of biodiesel is another challenge. The demand for a coating that not only enhances wear resistance but also aligns with sustainability goals is a critical problem that requires innovative and effective resolution. Therefore, the current drawbacks can be overcome via surface modification techniques that are capable of providing injector nozzle materials with a more resistant surface. The need to improve existing techniques to address

* Corresponding authors.
E-mail address: maleque@iium.edu.my (M.A. Maleque).

https://doi.org/10.1016/j.diamond.2024.111616
Received 8 June 2024; Received in revised form 8 September 2024; Accepted 24 September 2024
Available online 30 September 2024
0925-9635/

Fig. 1. Typical diesel engine injector nozzle with nozzle hole.

corrosion, wear, and friction issues is evident, emphasizing the urgency of developing enhanced surface modification solutions.

The injector nozzle materials are subjected to wear problems in the presence of biodiesel due to higher lubricity and higher oxygen content in biodiesel with increased surface interactions and material incompatibility leading to material degradation, corrosion, or increased susceptibility to mechanical wear. The deposition and wear phenomena, particularly in the injector nozzle materials, pose a critical problem that requires immediate attention. The main challenges are the wear and surface coking issues within biodiesel engine injector nozzle materials, resulting in an accelerated deposition rate of black smoke or black carbon within these systems when subjected to temperatures exceeding 300 °C. The nozzle surface is chemically degraded when the biodiesel and combustion products adhere to the internal surfaces of an injector. In recent years, research efforts have aimed at improving diesel engine designs for enhanced fuel efficiency and reduced emissions. The precise control of fuel injection pressure in the injector nozzle system of heavy trucks and motor vehicles was the focal point [6]. Yet, basic functional requirements such as machining injection holes to precise tolerances and resilience of materials to injector nozzle systems for better wear and fatigue resistance remain areas demanding further attention [7,8]. The content of sulfur in diesel fuel has a considerable influence, with low sulfur fuels showing instrumental in emission reduction. While low-sulfur fuels mitigate emissions, the sulfur-containing organic molecules in fossil fuels like gasoline and diesel contribute to environmental hazards such as acid rain, soil pollution, and harm to ecosystems and infrastructure [9].

The conventional coatings such as thermal barrier coating using partially stabilized zirconium and aluminium oxide [10], carbon-coating using plasma-assisted chemical vapor deposition [11] and ceramic coating with plasma spray technique [12] are used for automotive engine injector nozzles to improve wear resistance, reduce friction, and enhance the durability. The classical surface deposition method of CVD has been applied to the biodiesel engine components for various functions emphasizing on the biodiesel engine component damage [11] and found that the components were easily degraded by biodiesel fuel combustion leading to the formation of nozzle holes (as shown in Fig. 1) and damage of nozzle surface with various types of wear. There is no systematic and robust coating or surface modification method has been published in literature to prevent above-mentioned problem associated with bio-diesel operated injector in engine. On the other hand, this basic functional requirement has not yet fully addressed that the injector holes can be machined to close enough tolerances to provide the desired injection patterns and that the materials can withstand millions of combustion cycles and high-pressure pulses without yielding to fatigue damage of the component as well as without coking on the injector nozzle surface [13].

In the literature, studies focusing on friction-wear related problems in injector nozzle systems of internal combustion engines using diesel fuel (petroleum diesel and biodiesel) that have noted significant technological advancements in the design and material selection of injector systems. However, reducing or controlling the adverse effects of biodiesel on injector systems remains a challenge. The use of biodiesel (especially palm and soy oil-based biodiesel) as an alternative to petroleum diesel is noted for its advantages. Particularly, research and development, as well as practical applications, are intensively ongoing for solving issues related to friction-wear in sliding components of injector systems (injector needles, sockets), wear and coking problems on injector surfaces and fuel spray holes through surface coating treatments [14,15]. Therefore, it is highly demandable to develop a systematic and protective coating architecture on the injector surface with DLC approach in order to solve or minimize the problems with material incompatibility on biodiesel in new generation diesel engine.

DLC coatings, known as environmentally friendly thin film sustainable coating, offer a solution through thin film applications on many substrate materials and contribute to a greener environment by reducing friction, wear, fretting, galling, and corrosion of metallic substrates [15]. DLC thin film is synthesized using various deposition techniques such as plasma-assisted magnetron sputtering [16], pulsed laser deposition and cathodic arc deposition [17] and high power ımpulse magnetron sputtering (HiPIMS) [18]. Among these methods, the main advantages of HiPIMS coatings include a denser coating morphology, ease of control over deposition parameters, and uniform film homogeneity compared to conventional PVD coatings. The hydrogenated DLC coating is an amorphous carbon-based thin film with a sp^3 hybrid bond content below 70 % and a hydrogen content between 20 and 50 at. % is commonly referred to as a-C:H film and is known for its hardness and low friction. Research by Tanmaya et al. [19] investigates the tribological behavior of tetrahedral amorphous diamond-like carbon (ta-C DLC) coatings, emphasizing the occurrence of abrasive wear in non-conformal tribo-contacts. Another study focuses on hydrogenated metal-doped DLC coatings (Me-DLC, where Me = Al, Ti, or Nb) synthesized on AISI M2 steel substrate [20] and they claimed that the addition of Nb alters the coating's structure and reduce the residual stress leading to the better tribological properties. Nb-DLC coating is considered as one of the advanced form of DLC coatings, which improves the mechanical and tribological properties, making it more appropriate for some applications in automotive engines, aerospace components, and other high-stress mechanical systems where standard DLC coatings might fall short.

The literature suggests a persuasive description on the Nb-DLC coatings, indicating that the incorporation of Nb as a dopant in thin films provides radical effects on microstructural characteristics which in turn improve the adhesion property of the coated surfaces [21]. Specifically, this shift has revealed for developing a finer-grained, homogenous, and denser microstructure, thus improve the inherent quality of the films [22,23]. Furthermore, the doping of Nb appears as a catalyst in enhancing solid solution formation and supporting corrosion resistance, thereby leading to the enhancement of mechanical properties [24]. These meticulous insights from the literature emphasize the pivotal role of niobium doping for engineering thin films with superior structural integrity and functional performance. The findings highlight the dependency of coating properties on the metal content, with carbide-

Table 1
Variable parameters with levels and constant parameters used for Nb-DLC coating accepted the current state.

Variable parameters	Level 1	Level 2
Nb Target Current (A)	2	3
Duty Time (μs)	1	2
Bias Voltage (-V)	50	100

Constant parameters	
Cr Interlayer current (A)	3
Cr Interlayer time (min.)	10
C Target Current (A)	0.5
Deposition Pressure (Pa)	0.26
C_2H_2 Flow Rate (sccm)	17
Frequency (kHz)	100
Nb-DLC layer time (min.)	70

Table 2
Taguchi experiment parameters for Nb-doped DLC coating.

Sample ID[a]	Nb target current (A)	Duty time (μs)	Bias voltage (-V)
R1-A and B	2	1	50
R2-A and B	2	2	100
R3-A and B	3	1	100
R4-A and B	3	2	50

[a] R1-, R2-, R3-, and R4-A runs for H13 steel; R1-, R2-, R3-, and R4-B runs for AISI 420 SS.

forming solid metals playing a leading role in controlling the tribological properties of the DLC-coated M2 grade tool steel [20]. The current study focuses Nb-DLC coatings as a more advanced alternative to conventional DLC coatings, addressing the specific challenges posed by biodiesel environments. Previous work by İhsan Efeoğlu and his research team extensively examined both undoped and doped DLC coatings across various applications [25–28], highlighting DLC's potential. However, under the demanding conditions experienced by biodiesel injector nozzles, where high wear resistance and corrosion protection are critical, the standard undoped DLC coatings often exhibit limitations in long-term durability and performance. The incorporation of Nb enhances the mechanical and tribological properties of DLC, particularly by improving wear resistance making Nb-DLC a more suitable option for such demanding environments. Therefore, this study's focus on Nb-DLC represents a natural progression based on cumulative research findings, offering a more suitable solution for applications in biodiesel injector systems.

Despite many efforts, minimal attention has been paid to the Nb-doped DLC coating for biodiesel injector nozzle materials such as AISI 420 stainless steel and H13 tool steel to prevent the unanticipated damage of the fuel injector system materials in presence of biodiesel. The specific focus of this study is to investigate the thin film coating characteristics and tribological performance of Nb-DLC coatings on H13 tool steel and AISI 420 SS. Therefore, the research aims to synthesize Nb-DLC Coatings employing the CFUBMS technique to deposit Nb-DLC coatings on both materials followed by the characterization of the coatings and optimization of the coating process parameters utilizing Design Expert software and Taguchi design of experiments to determine the optimal coating process parameters. Moreover, the Nb-DLC coating using a CFUBMS system with its functionally designed architectural has been introduced in the current study to prevent the coking and deposition formation on the nozzle surface due to biodiesel combustion. The novelty of using Nb-DLC coatings on injector nozzle materials are the enhancement of hardness and tribological properties. It is believed that this enhancement can significantly extend the lifespan of injector nozzles in biodiesel environments. Therefore, this study addresses the synthetization of a hydrogenated Nb-doped DLC coating on commonly used two types of biodiesel injector materials. The investigation explores structural, mechanical, and tribological properties, employing advanced techniques such as Raman spectroscopy, XRD, micro-hardness, and pin-on-disc testing.

2. Experimental

The experiments began with the deposition of Nb-doped DLC thin film coatings on four different substrates of H13 steel, AISI 420 stainless steel (SS), and glass materials. This was achieved by CFUBMS technique, employing a cutting-edge UDP550-type coating rig. Table 1 summarizes both variable and constant parameters instrumental in the deposition process. Meanwhile, Table 2 presents the formulation of samples aligned with the CFUBMS parameters to run the experiment based on the stated parameters to investigate the effect of those parameters on the thin film coating performance. Also, this Table 2 represent the utilization of Taguchi design of experiments to optimize the coating process parameters. Fig. 2 represents a visual guide depicting the CFUBMS pattern of the utilized targets and the architectural structure of the Nb-doped DLC thin film coatings. The surface preparation of H13 steel and AISI 420 SS substrates was performed using a rigorous ultrasonic cleaning process, followed by polishing with 400, 600, 800, and 1200 grits abrasive paper, resulting in surface roughness values of 0.02 μm (R_a).

The thin film coating process was done on substrate materials, utilizing two Nb targets (99.95 % pure), one Cr target (99.95 % pure), and one C target (99.95 % pure). The Advanced Energy Pinnacle Plus pulsed-DC power supply was integrated with the Nb targets, while an Advanced Energy Pinnacle DC power supply was incorporated for the Cr and C targets. The gas ratios of two gases (Ar and N2) were managed by mass flow controllers (MKS system) for better control of the gas and a balanced environment within the deposition chamber. The substrates were affixed to the plasma chamber system that elegantly rotated (one-degree rotation), positioned strategically in front of the targets. The distance between the substrates and the targets was 70 mm at the closest point.

Before the thin film coating process, ion cleaning occurred within the plasma chamber for 30 min. Ar gas was utilized under an 800 V negative bias voltage (DC) to purge any remaining contaminants, setting the stage for optimal adhesion between the substrate and the film [23]. The Cr interlayer was deposited for 10 min to further enhance the adhesion between the substrate and the Nb-thin film coating by effectively grading the film from a metallic layer to a ceramic layer without an abrupt transition. During the deposition of the Cr interlayer, the current applied to the Cr targets was fixed at 3A for the entire film formation as shown in Table 1. The Cr was deposited from the Cr target as shown in Fig. 2(a).

Then, the Nb-doped DLC coating deposition was developed for 90 min. The parameters outlined in Table 2 served as the guiding script for this DLC coating development. The Nb-doped DLC coating then undergoes various characterizations. The Raman spectra were used for composition and structure using a 532 nm wavelength laser via a WITech alpha 300R Micro Raman Spectrometer. The crystal structures were extracted from thin films deposited on Si substrate using XRD, employing a Rigaku DMax-2200 type with Cu-Kα radiation source and a 30–100° scan range.

The micro-hardness of the thin films was measured with a Buehler Micromet 2001 Microhardness tester. The micro-hardness test was conducted using a Knoop indenter and a $10g_f$ load applied for 15 s (an indentation delay). The critical load values, indicating the coating's adhesion strength, were determined on a CSM Instruments scratch tester (Revetest Xpress), applying a progressive load of 0-80 N. The wear and friction of the Nb-DLC coated materials were assessed under specific conditions, including a 2 N load, 10 cm/s velocity, and a 6.25 mm diameter Al2O3 counterpart, using the CSM tribotester (Tribometer THT S/N 11–175) system. These parameters allowed for a comprehensive

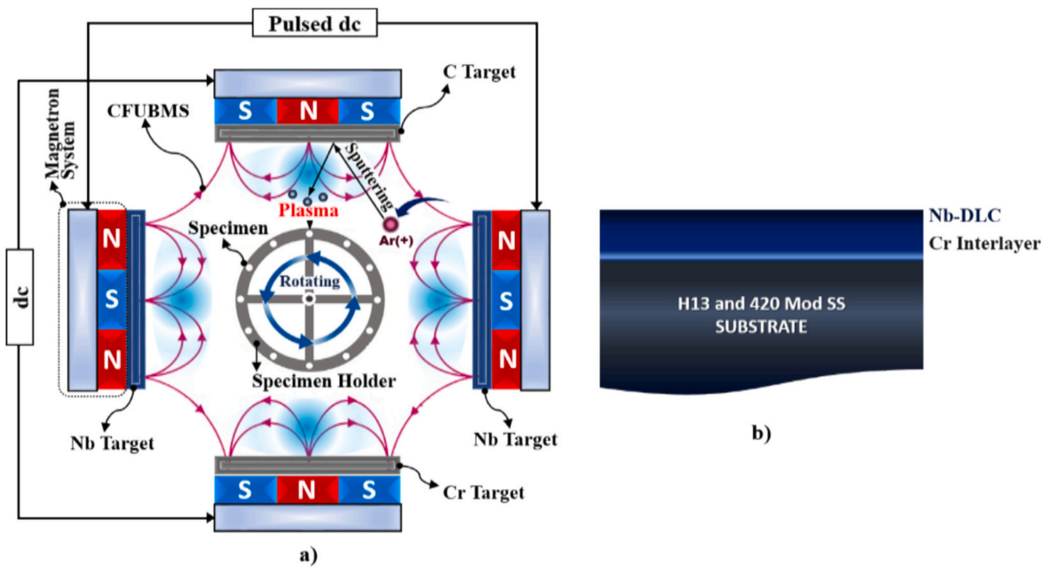

Fig. 2. a) Closed Field Unbalanced Magnetron Sputtering (CFUBMS) system and b) The arhitecture of Nb-DLC thin film coating.

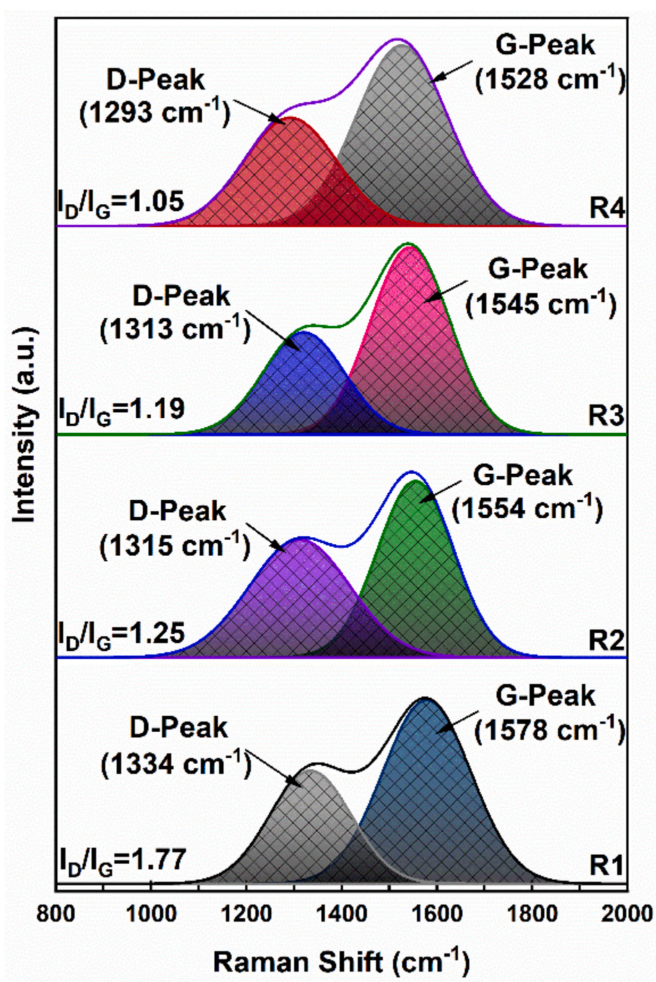

Fig. 3. Raman spectrum (deconvolution) of Nb-doped DLC coating collected at various deposition parameters as mentioned in Table 2 for R1, R2, R3 and R4 runs.

understanding of the coatings' wear and frictional properties and their potential applications in the tribological field.

3. Result and discussion

3.1. Structure of Nb-DLC coatings

Employing Raman spectroscopy as a dedicated tool for structural characterization of Nb-doped hydrogenated DLC coatings, the study explores the differences between diamond and graphite structures within the outer carbon layer of these new coatings. Fig. 3 presents the Raman spectra derived from Nb-doped DLC thin film coatings on the glass substrate, each corresponding to distinct deposition parameters in the R1, R2, R3, and R4 runs. The spectral data, covering a range of 800–2000 cm^{-1}, underwent particular deconvolution using two Gaussian fits—D and G peaks—via OriginPro 2022 (Version 9.9.0.225). Raman spectroscopy revealed a shift in the peaks identified as D and G peaks in the structures, as shown in Fig. 3. In general, G peaks are associated with graphite-like sp^2 bonds apparent near 1580 cm^{-1} in Nb-DLC coatings, while D peaks indicative of diamond-like sp^3 bonds surface around 1350 cm^{-1} [29].

In this investigation, G peaks positioned themselves at wave numbers of 1578, 1554, 1545, and 1528 cm^{-1} for the R1, R2, R3, and R4 films, respectively. Simultaneously, D peaks imprinted their identity at wave numbers 1334, 1315, 1313, and 1293 cm^{-1} for the corresponding runs. The correlation of sp^3/sp^2 bonding ratios with the G- and D-peaks, along with integrated intensity ratios (ID/IG), provided valuable insights into the intricate composition of these coatings.

The typical shifts observed in both D and G Raman peaks across varying CFUBMS process parameters during DLC coating highlight the dynamic nature of these coatings. Notably, the ID/IG ratio exhibited a noticeable decrease with the increase of both Nb target current and bias voltage, revealing a pivotal interplay between process parameters and the structural composition of Nb-doped DLC coatings. It can be concluded that analysis extends the structural distinctions within Nb-doped DLC coatings and the dynamic nature of these coatings in response to intricate DLC deposition parameters. Fig. 3 also visually reinforces the inverse relationship between the ID/IG ratio and the increasing Nb target current and bias voltage.

Fig. 4 presents the computed averages for the ID/IG ratio, a pivotal metric where a 'smaller is better' for the response calculation. The determination of these averages was accurately conducted through the

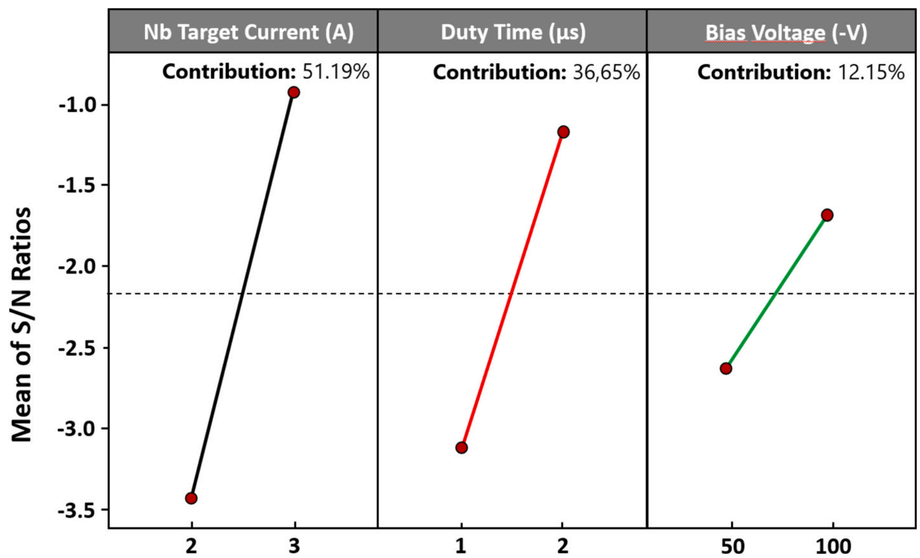

Fig. 4. Mean effects plot for S/N ratios of ID/IG ratio Nb-doped DLC thin film coatings.

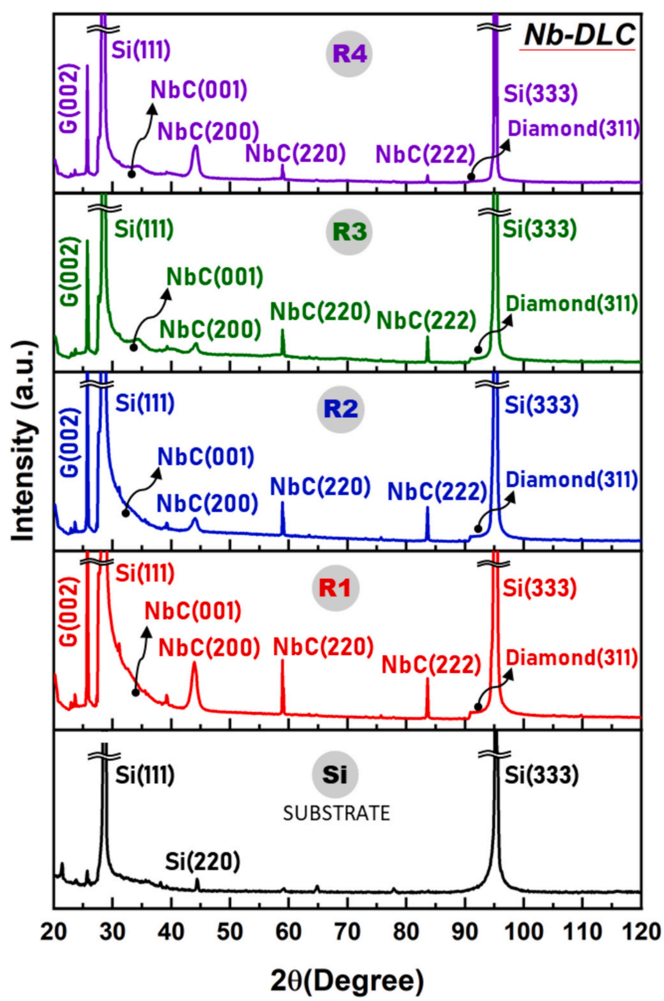

Fig. 5. XRD graphs of Si substrate and Nb-DLC hydrogenated coated Si.

Taguchi Design of Experiments (DOE) methodology, utilizing Minitab software in its 21.3.1 version. In order to distinguish the impact of various process parameters on the ID/IG ratios, a comprehensive Analysis of Variance (ANOVA) was undertaken. The results, depicted in Fig. 4, revealed the distinct contributions of Nb target current, duty time, and bias voltage to the ID/IG ratios within Nb-doped DLC films. Particularly, the ANOVA results portray a significant control, with Nb target current accounting for 51.19 %, followed by duty time with 36.65 %, and bias voltage contributing 12.15 % to the overall variability in the ID/IG ratios.

The Nb target current parameter is the most influential factor in achieving structural distinctions within Nb-doped DLC coatings, as shown in Fig. 4, which represents the mean response for the S/N ratio of structural characterization of Nb-doped hydrogenated DLC coatings. Other important factors, in order of influence, include duty time and bias voltage. This distinguished breakdown serves as a key analytical insight into the complex interaction of these process parameters and their respective influence on the ID/IG ratios in Nb-doped DLC films.

3.2. XRD analysis

The crystalline phase of Nb-doped hydrogenated DLC thin film-coated Si substrate was investigated using an XRD analyzer. Fig. 5 presents a comprehensive XRD graph, illuminating the crystalline landscape and representing the distinctive insights of the structural phases.

In the XRD spectra, noticeable peaks attributed to the Si substrate stand prominently, with Si (111), Si (220), and Si (333) peaks [30–32]. Beyond the Si substrate peaks, the runs of R1, R2, R3, and R4 exhibited additional peaks, including G (graphitic carbon) (002), NbC (001), NbC (200), NbC (220), and NbC (222) [14,33,34]. The Si (111) and Nb (001) peaks for R1, R2, R3, and R4 runs showed the exact value shifting of the reflection angle resulting in a phenomenon of peak broadening. The XRD graphs further highlight the occurrence of a diamond (311) peak proximate to the Si (333) peak for R1, R2, and R3 runs, leading to a distinct broadening on the left side of the Si (333) peak [35,36]. This observation signifies the integral role of diamond structures in increasing the Nb-DLC coatings' hardness and wear resistance. Essentially, Nb doping in the coating structure leads to the formation of NbC phase, rather than Nb being present in its pure form. However, the XRD peaks predominantly demonstrate the formation of the diamond and NbC structure. This is consistent with the findings of another publications [14], whereby XRD peaks were identified as NbC in Nb-doped coatings. The influence of diamond structures, graphitic carbon, and NbC across all coating structures collectively improve the hardness and tribological properties [34–36].

The XRD analysis of amorphous hydrogenated diamond-like carbon (a-C:H) coatings often yields limited information on the phase

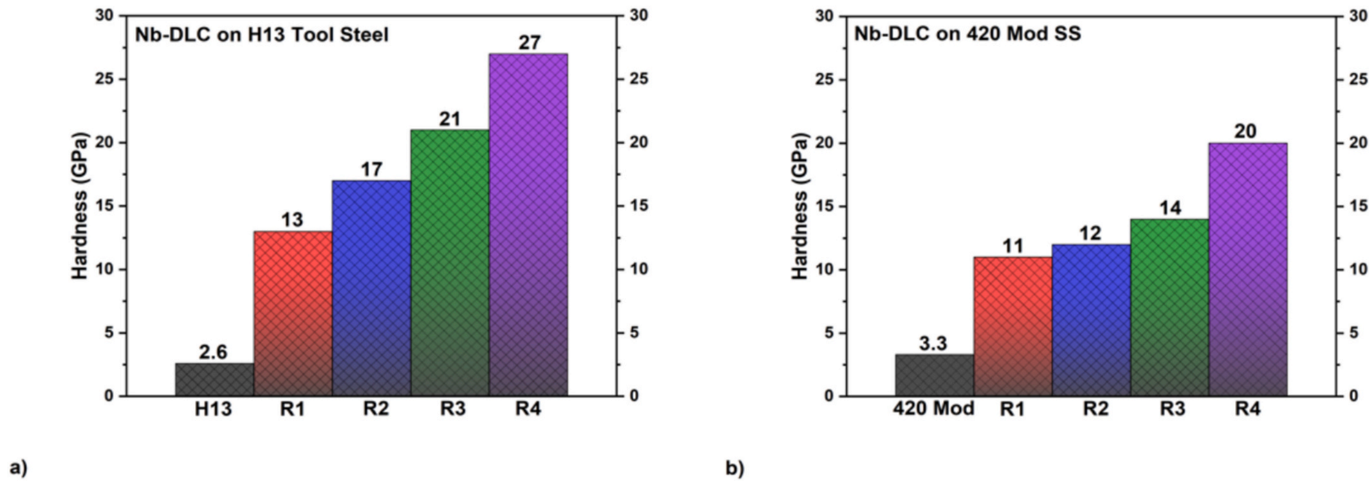

Fig. 6. Microhardness values of Nb-DLC coated injector materials: a) H13 tool steel and b) AISI 420 SS material.

identification due to their amorphous nature and the presence of a broad hump instead of distinct peaks. The conventional XRD technique exhibited lack of long-range order of a-C:H films and hence, Si substrate was chossen for a meaningful structural insights. The diffraction analysis conclusively establishes a notable occurrence of diamond structures in the DLC coating, employing a reflective impact on enhancing hardness and wear resistance. The significance of prior research is noteworthy, affirming the positive correlation between preferred diamond structure and higher hardness, particularly under higher bias voltage [37]. It can be concluded that the XRD analysis demonstrates the elaborate crystalline phases within Nb-DLC coatings, which substantiates their potential as robust candidates for biodiesel injector materials, affirming their resilience in the context of wear and tribological challenges.

3.3. Hardness properties

Micro-hardness values determined using the Knoop microhardness technique are presented in Fig. 6, which is considered as one of the most reliable methods for evaluating thin film hardness. The Knoop method is particularly advantageous for thin films due to its elongated indent shape, which minimizes substrate effects compared to other microhardness testing methods. Given the significant penetration depth, there is an increased likelihood that the measured hardness values may be influenced by the substrate material. Therefore, multiple tests were conducted for each test run at loads exceeding 10 g to ensure accurate and consistent results.

The maximum hardness value obtained for Nb-doped DLC coating of 27 GPa for R4 run on H13 and 20 GPa for R4 run on AISI 420 SS. The difference in hardness between Nb-DLC-coated H13 steel and AISI 420 SS can be attributed to the properties, composition, and coating process response to the substrate. DLC coating developed with the highest Nb target current demonstrated superior hardness compared to other variable parameters, as stated in Table 2. This enhanced hardness could be attributed to the amplified solid solution strengthening effect on the coating with an increased Nb target current. The elevated target current and duty cycle might have resulted in a denser, finer-grained coating.

As mentioned earlier, the XRD diffraction analysis of the R4 run revealed a prominent growth of graphitic carbon (002), NbC (001), NbC (200), NbC (220), and NbC (222) phases. The Nb-DLC coating introduces niobium into the DLC structure, known for its exceptional hardness, wear resistance, and low friction properties [17,18]. However, when the target current and duty cycle are more downward (Table 2), the preferred orientation shifts from left to right, decreasing the hardness of the Nb-DLC coating.

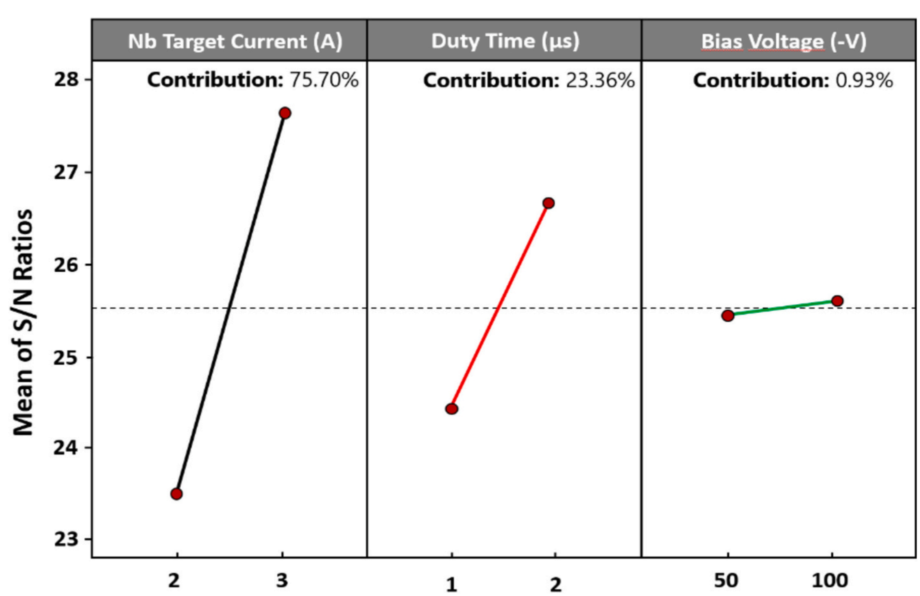

Fig. 7. Mean effects plot for S/N ratios of hardness of Nb-doped DLC thin film coatings.

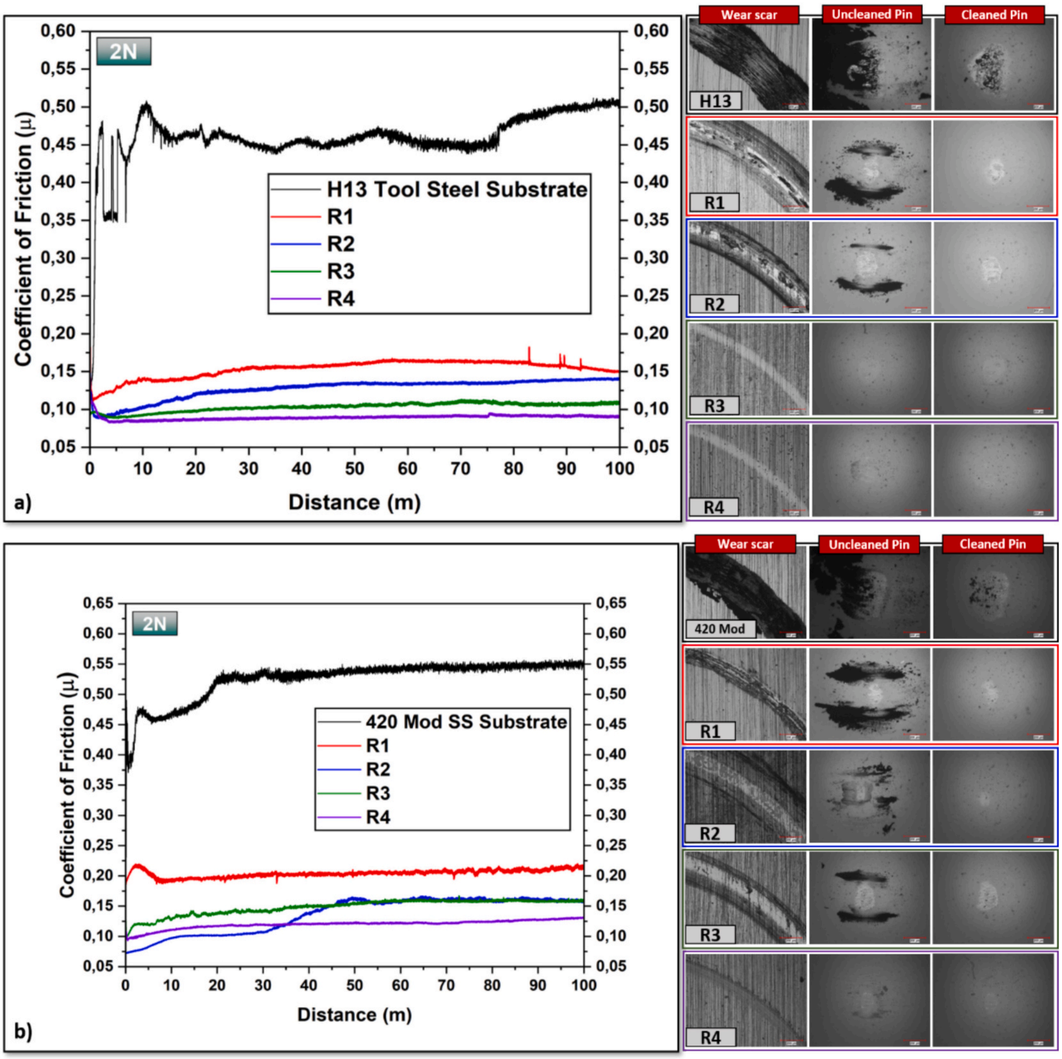

Fig. 8. Friction coefficient along with optical microscopy image on wear damage surface of Nb-DLC coated injector materials: a) H13 tool steel and b) AISI 420 SS material.

The presence of NbC (200) and diamond (311) structures significantly influenced the hardness values, particularly in the R4 run, where the highest hardness value of 27 GPa attained on H13 steel. The combination of chromium, molybdenum, vanadium, and other elements in H13 steel exhibited a better response to the coating, allowing better adhesion and performance than AISI 420 SS. This suggests that the composition and microstructural arrangement of the coatings played a vital role in influencing their hardness property. In summary, the findings of the structure and XRD reflection peak patterns have provided valuable insights into the influence of variable parameters on the Nb-DLC coatings.

Fig. 7 presents the computed average levels for the for the hardness value of Nb-doped DLC coating, a pivotal metric where a 'larger is better' for the response calculation, offering a meticulous view on the performance metric. The determination of these averages was accurately conducted through the Taguchi Design of Experiments (DOE) methodology, utilizing Minitab software in its 21.3.1 version. In order to assess the meticulous impact of various process parameters on the hardness value, a comprehensive Analysis of Variance (ANOVA) was undertaken. As illustrated in Fig. 7, the ANOVA results reveal the distinct contributions of Nb target current, duty time, and bias voltage to the hardness value within Nb-doped DLC films. Particularly, these results outline a considerable hierarchy, with Nb target current proclaiming a leading influence at 75.70 %, followed by duty time at 23.36 %, and bias voltage contributing a marginal 0.93 % to the overall variability in the hardness value. This analysis provides a reflective analytical insight into the complex impact of various process parameters, shaping the hardness value in Nb-doped DLC films.

3.4. Friction and wear performance

The friction and wear performance tests of Nb-doped hydrogenated DLC thin film coated H13 tool steel and AISI 420 SS were performed using a pin-on-disc tribometer, and Fig. 8 shows the friction coefficient along with the wear damage surface of Nb-DLC coated injector materials. The test was conducted over a traversed distance of 100 m under an applied load of 2 N.

In Fig. 8a, the Nb-DLC coatings on H13 steel demonstrated a friction coefficient approximately four times lower than the H13 substrate. A trend of tribological dynamics is disclosed—embarking with a run-in period for the initial 5 m, followed by stable friction with an average coefficient of 0.10 for Run 4 throughout the experimental period. The optical microscope image of the pin (Al2O3) and H13 and Nb-DLC coated H13 steel are also shown in Fig. 8a. Based on the optical microscope images, it is evident that the damaged surface showed very minimum wear debris particles and narrower width of wear scar resulting lower friction coefficient (especially for R4 run). Additionally, the Nb-DLC coating remained intact on the surface throughout the

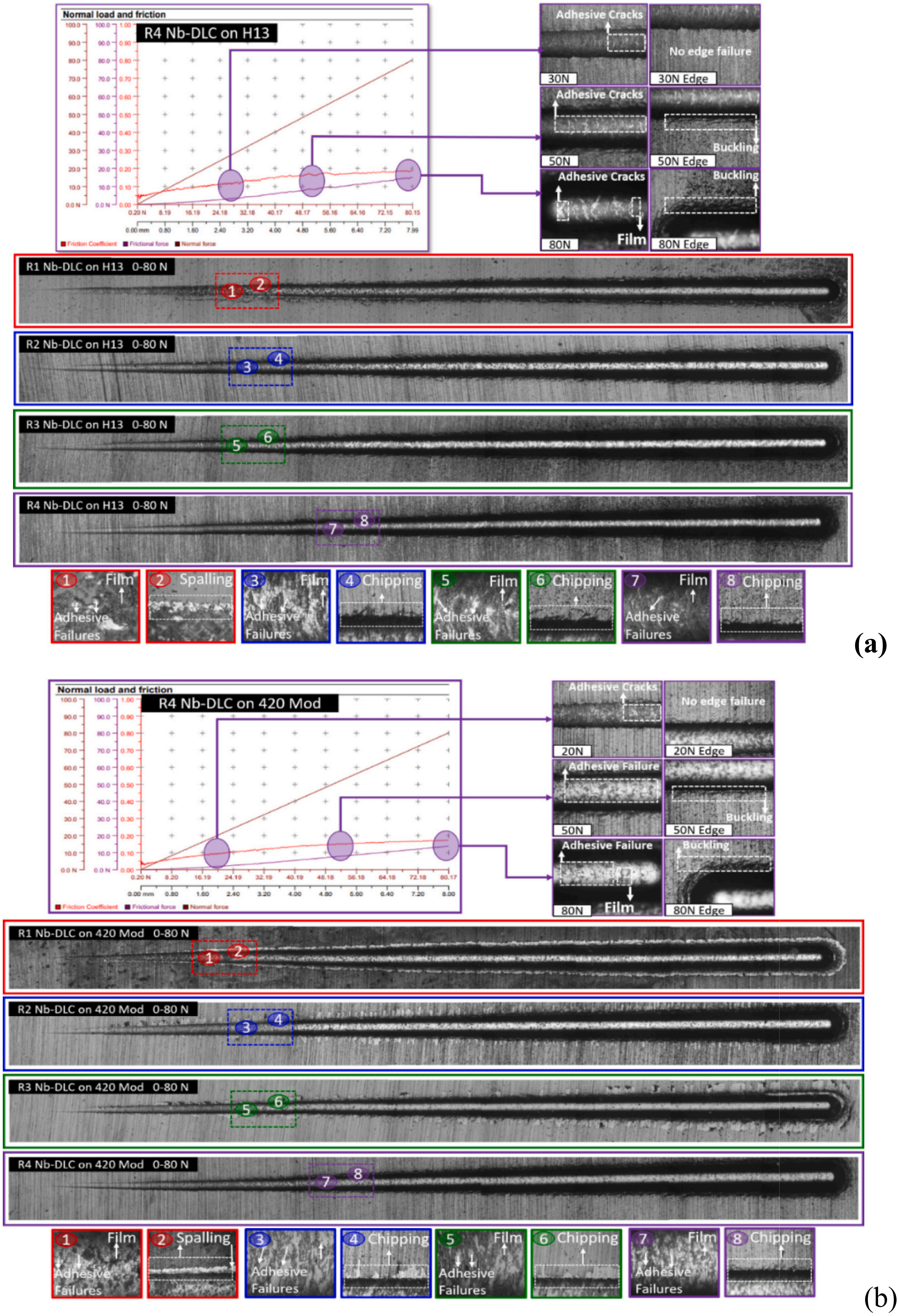

Fig. 9. Scratch images of Nb-DLC coated injector materials within the 0–80 N progressive load: a) H13 tool steel and b) AISI 420 SS material.

experiment due to the higher hardness value attainment (as explained earlier). The friction coefficient of Nb-DLC coated H13 steel exhibited significant improvement with the lowest value of 0.10 as compared to 0.52 for the substrate material, underscoring the transformative impact of Nb-DLC coatings on the frictional properties of H13 tool steel.

Fig. 8b shows the friction coefficient results of Nb-DLC coating on AISI 420 SS and substrate material. The friction coefficient values of Nb-DLC coatings on AISI 420 SS also revealed a more or less stable behavior. They showed an improvement almost similar to the results obtained from H13 steel. Again, the lowest friction coefficient for Nb-DLC coating on AISI 420 SS was achieved in the R4 run due to an eloquent expression of the highest film hardness value of 20 GPa. As hardness increases, the coefficient of friction decreases due to the reduction of adhesiveness and deformation of the mating surfaces. The deformation of the mating surface directly influences the adhesive element of friction. It is well-known that hard materials, due to their atomic solid bonds and surface energy, exhibit enhanced adhesion resistance, resulting in reduced friction coefficient values [38–40]. It can be concluded that the Nb-DLC coatings on the substrate revealed a transformative impact of hardness on friction and wear performance.

3.5. Adhesion property

The adhesion properties of the Nb-DLC coatings were evaluated using the CSM Instruments scratch tester, and the results are shown in Fig. 9. A progressive load in the range of 0–80 N was applied to the coatings, and the scratch behavior was investigated. Fig. 9(a) presents the scratch images of Nb-DLC thin film-coated H13 steel for R1, R2, R3 and R4 runs. In contrast, a separate friction coefficient vs normal load profile and scratch image of the R4 run is depicted on top of the four samples (as this R4 run showed better hardness, friction, and wear performance). Upon examination of Fig. 9(a), the critical load of Nb-DLC coated injector materials for R1, R2 and R3 runs was monitored. The coating detached from the substrate at a load of 80 N. Particularly, the R4 run exhibited a unique resilience, with the coating remaining steadfastly adhered to the substrate beyond the critical load, demonstrating its superior scratch behavior or adhesion behavior with higher critical load value. After the 30 N load value, spalling, adhesive cracks, and chipping increased for R1, R2 and R3, causing the coating to separate from the substrate. In contrast, the R4 run showed no flaking/chipping but mild adhesive cracking until reaching the critical load value, as captured in the top right corner of Fig. 9(a). This study's scratch surface images witness spalling, adhesive cracks, and chipping, aligning with prior research findings [29].

Fig. 9(b) shows the scratch images of Nb-DLC thin film coated AISI 420 SS for R1, R2, R3 and R4 runs whereas, a separate friction coefficient vs normal load profile within the range of 0–80 N as well as the image of R4 run depicted on top of the four samples. Here, the adhesion behavior is revealed at a different pace. The adhesion behavior of the Nb-DLC coated AISI 420 SS at an 80 N load value showed a more noticeable weakness in adhesion surfaces. The scratch-damaged surfaces of R1, R2, and R3 runs reveal a significantly different adhesion from H13 steel. Meanwhile, the R4 run presents a delicate shift, with buckling edge damage evolving as a distinctive feature. In addition, spalling, adhesive cracks, and chipping edge damage [41,42] were observed in the R1, R2, and R3 runs, while buckling edge damage was noticed in the R4 run.

4. Conclusions

This investigation articulated the synthesis of Nb-DLC thin film coatings, upon two distinct biodiesel injector nozzle materials using the CFUBMS technique. The comprehensive characterization of the Nb-DLC hydrogenated thin film coating encompassed assessments of structural composition, crystalline phases, hardness, friction coefficients, and critical load measurements. Structural analysis revealed the presence of G peaks, indicative of graphite-like sp^2 bonds at approximately 1580 cm^{-1} within Nb-DLC coatings, while D peaks associated with diamond-like sp^3 bonds manifested around 1350 cm^{-1}. This meticulous structural distinctions highlighted the intricate dynamics inherent to Nb-doped DLC coatings in response to deposition parameters. XRD analysis further elucidated the composition, exhibiting phases such as graphitic carbon (002), NbC (001), NbC (200), NbC (220), NbC (222), and the appearance of a diamond (311) phase on the Nb-DLC coatings. The shifting of Nb (001) peaks in correlation with reflection angles featured the role of diamond structures in enhancing the hardness and wear resistance of Nb-DLC coatings. Results showcased that Nb-DLC coated H13 steel exhibited superior hardness (27 GPa) and lower friction coefficient (0.10) compared to AISI 420 SS material (20 GPa and 0.21, respectively), demonstrating the consequential impact of deposition parameters such as a target current of 3 A, duty time of 2 microseconds, and a bias voltage of −100 V. This collective improvement in structural properties contributes significantly to the hardness of Nb-DLC-coated injector materials.

Scratch test results demonstrated superior adhesion properties of Nb-DLC-coated injector nozzle materials of H13 steel compared to AISI 420 SS material exhibiting higher critical load values. Therefore, the adhesion behavior of Nb-DLC-coated AISI 420 SS at an 80 N load exhibited noticeable weakness in adhesion compared to H13 steel. In conclusion, the consolidation of higher hardness, improved coating crystallinity, and enhanced adhesion properties of Nb-DLC-coated H13 steel injector nozzle materials positions them as promising candidates for facilitating the sustainable integration of biodiesel in automotive engines.

Funding

This research was supported by The Coordination Unit of Scientific Research Projects (Project ID: FKP-2022-10687), Ataturk University, Turkey.

CRediT authorship contribution statement

Ihsan Efeoglu: Investigation, Funding acquisition, Conceptualization. **Md Abdul Maleque:** Writing – original draft, Methodology, Conceptualization. **Gokhan Gulten:** Writing – original draft, Funding acquisition, Formal analysis, Data curation. **Mustafa Yesilyurt:** Visualization, Investigation. **Banu Yaylali:** Visualization, Investigation. **Yasar Totik:** Writing – review & editing, Methodology. **Md Abul Kalam:** Writing – review & editing, Formal analysis. **Masjuki Haji Hassan:** Writing – review & editing, Supervision. **Nurin Wahidah Zulkifli:** Writing – review & editing, Methodology.

Declaration of competing interest

The authors declare that they have no known competing financial interests or personal relationships that could have appeared to influence the work reported in this paper.

Data availability

The dataset produced and analyzed during the study is available with me as the corresponding author, contingent upon obtaining consent from all the authors involved. The data cannot be publicly accessed due to its intended publication through a reputable journal. However, should the Editorial team require access to the data, I am fully prepared to provide it on behalf of all the authors.

Acknowledgments

The authors would like to thank Ataturk University for funding the project. The corresponding author (M A Maleque) thanks the Scholarship and Study Leave Committee of the Management Service Division, International Islamic University of Malaysia (IIUM), for giving him research leave. The authors are also grateful to the IIUM, University of Technology Sydney, Australia, and University of Malaya (Malaysia) for supporting this study. The financial support for the journal APC from University of Technology Sydney, Australia is also greatly acknowledged.

References

[1] P. Pablo-Romero, R. Pozo-Barajas, J.G. Sánchez, J.L. Holechek, H.M. Geli, R. Sawalhah, M.N. Valdez, A global assessment: can renewable energy Rrplace fussil Ffels by 2050? Sustainability 14 (4792) (2022) https://doi.org/10.3390/su14084792.
[2] M. Gulzar, H.H. Masjuki, M. Varman, M.A. Kalam, N.W.M. Zulkifli, R.A. Mufti, A. M. Liaquat, R. Zahid, A. Arslan, Effects of biodiesel blends on lubricating oil degradation and piston assembly energy losses, Energy 111 (2016) 713–721, https://doi.org/10.1016/J.ENERGY.2016.05.132.
[3] I. Kralova, I.J. Sjöblom, Biofuels-renewable energy sources: a review, J. Dispers. Sci. Technol. 31 (2010) 409–425, https://doi.org/10.1080/01932690903119674.
[4] A.T. Doppalapudi, A.K. Azad, M.M. Khan, Advanced strategies to reduce harmful nitrogen-oxide emissions from biodiesel fueled engine, Renew. Sustain. Energy Rev. 174 (2023) 113123, https://doi.org/10.1016/J.RSER.2022.113123.
[5] A.T. Hoang, A.T. Le, A review on deposit formation in the injector of diesel engines running on biodiesel, Energ Source Part A. 41 (2019) 584–599, https://doi.org/10.1080/15567036.2018.1520342.
[6] H. Thomas, S. Stefan, T. Andrew, S. Stephen, D. John, A benchmark study on the flow metering systems for the characterisation of fuel injectors for future heavy duty commercial vehicles, Measurement 153 (2020) 107414, https://doi.org/10.1016/j.measurement.2019.107414.
[7] H. Ogawa, K. Mori, T. Ishikawa, Y. Kobashi, G. Shibata, Improvement of diesel combustion with suppression of mutual fuel spray flame interactions with staggered nozzle hole arrangement and a spatially divided combustion chamber, Int. J. Engine Res. 24 (9) (2023) 4276–4286, https://doi.org/10.1177/14680874231191563.
[8] H. Jia, Y. Jian, B. Yin, J. Yang, Z.Z. Liu, Experimental study on the combustion, emissions and fuel consumption of elliptical nozzle diesel engine, Energy 262 (2023) 125449, https://doi.org/10.1016/J.ENERGY.2022.125449.
[9] R.Y. Mamuad, R. Y., A.E.S. Choi, Biodesulfurization processes for the removal of sulfur from diesel oil: a perspective report, Energies 16 (2023) 2738, https://doi.org/10.3390/EN16062738.
[10] G. Suresh, H.C. Kamath, N.R. Banapurmath, M. Bhovi, Comparative study on effect of blending, thermal barrier coating (LHR) and injector nozzle geometry on biodiesel-fuelled engines, International Journal of Sustainable Engineering 9 (3) (2016) 206–214, https://doi.org/10.1080/19397038.2015.1128493.
[11] J. Hershberger, J.B. Woodford, A. Erdemir, G.R. Fenske, Friction and wear behavior of near-frictionless carbon coatings in formulated gasolines, Surf. Coat. Technol. 183 (2004) 111–117.
[12] R. Thirunavukkarasua, M. Mahendrana, R. Tamilselvana, S. Periyasamy, Investigation on single, four and five holes fuel ınjector nozzle on performance and emission characteristic of diesel on a vcr engine by using ceramic coating material on the piston crown, Materials Today: Proceedings 5 (2018) 7577–7585.
[13] Z.A. Hartono, B. Cahyono, Effect of using B30 palm oil biodiesel to deposit forming and wear metal of diesel engine components, International Journal of Marine Engineering Innovation and Research 5 (1) (2020) 10–19.
[14] S.S. Gautam, R. Singh, M. Feroskhan, Thermal barrier coatings for internal combustion engines: a review, Materials Science Engineering (2021), https://doi.org/10.1016/j.matpr.2021.10.371.
[15] B. Breidenstein, B. Denkena, P. Wolters, M. Keitel, W. Tillmann, D. Stangier, N. F. Lopes Dias, A novel development of sustainable cutting inserts based on PVD-coated natural rocks, Materials Today Sustainability 24 (2023) 100507, https://doi.org/10.1016/j.mtsust.2023.100507.
[16] D.F. Franceschini, Growth, structure, and properties of plasma-deposited amorphous hydrogenated carbon–nitrogen films, Thin Films and Nanostructures. 30 (2002) 217–276, https://www.sciencedirect.com/topics/materials-science/amorphous-hydrogenated-carbon.
[17] Ming-Chieh Chiu, Wen-Pin Hsieh, Wei-Yu Ho, Da-Yung Wang, Fuh-Sheng Shieu, Thermal stability of Cr-doped diamond-like carbon films synthesized by cathodic arc evaporation, Thin Solid Films 476 (2) (2005) 258–263, https://doi.org/10.1016/j.tsf.2004.09.029.
[18] Ji Cheng Ding, Wei Dai, Teng Fei Zhang, Pin Zhao, Je Moon Yun, Kwang Ho Kim, Qi Min Wang, Microstructure and properties of Nb-doped diamond-like carbon films deposited by high power impulse magnetron sputtering, Thin Solid Films 663 (2018) 159–167, https://doi.org/10.1016/j.tsf.2018.07.012.
[19] M.B. Tanmaya, D. Svanbäck, S. Tervakangas, B. Prakash, The effects of contact configuration and coating morphology on the tribological behaviour of tetrahedral amorphous diamond-like carbon (ta-C DLC) coatings under boundary lubrication, Tribol. - Mater. Surf. Interfaces (2019) 1–10, https://doi.org/10.1080/17515831.2019.1596627.
[20] I. Bouabibsa, S. Lamri, F. Sanchette, Structure, mechanical and tribological properties of Me-doped diamond-like carbon (DLC) (Me = Al, Ti, or Nb) hydrogenated amorphous carbon coatings, Coatings 8 (10) (2018) 370, https://doi.org/10.3390/coatings8100370.
[21] A.W. Zia, Z. Zhou, L.K. Li, Structural, mechanical, and tribological characteristics of diamond-like carbon coatings, Nanomaterials-Based Coatings (2019) 171–194, https://doi.org/10.1016/B978-0-12-815884-5.00007-7.
[22] Z.T. Wu, Z.B. Qi, D.F. Zhang, B.B. Wei, Z.C. Wang, Evaluating the influence of adding Nb on microstructure, hardness and oxidation resistance of CrN coating, Surf. Coat. Technol. 289 (2016) 45–51, https://doi.org/10.1016/j.surfcoat.2016.01.047.
[23] B. Yaylali, G. Gulten, I. Efeoglu, Y. Totik, P. Kelly, J. Kulczyk-Malecka, Influence of Nb and ta on the corrosion and mechanical properties of CrYN coatings, Surf. Coat. Technol. 476 (2024), https://doi.org/10.1016/j.surfcoat.2023.130249.
[24] M.A. Polat, G. Gökhan, T. Yaşar, et al., Synthesis and characterization of Ta/TaN coatings with CFUBMS-HiPIMS technology, in: M.A. Maleque, A.Z. Ahmad, N. Sarifuddin, et al. (Eds.), Proc. of 5th Int. Conf. on Adv. in Manuf. and Mat. Eng.: Lec. Notes Mech. Eng, 2023, p. 37.
[25] E. Arslan, Y. Totik, I. Efeoglu, I., The investigation of the tribocorrosion properties of DLC coatings deposited on Ti6Al4V alloys by CFUBMS, Prog. Org. Coat. 74 (4) (2012) 768–771.
[26] A.F. Yetim, A. Alsaran, A. Celik, I. Efeoglu, Corrosion behaviour of Ti DLC deposition on prenitrided 316L stainless steel and Ti–6Al–4V alloy, Corros. Eng. Sci. Technol. 46 (4) (2011) 439–444.
[27] F. Bülbül, I. Efeoğlu, The effect of TiC transient layer on a DLC-based functionally gradient coating prepared by closed field unbalanced magnetron sputtering plating system, Met. Mater. Int. 16 (2010) 573–580.
[28] I. Efeoglu, O. Baran, G. Urvasızoğlu, A. Keleş, M. Atatol, Y. Totik & U. Ertaş. The structural properties of Ta doped DLC coatings for the dental applications using HiPIMS. Solid State Sci. Technol, 27, (2029) 68–74.
[29] N. Sunthornpan, S. Watanabe, N. Moolsradoo, Elements-added diamond-like carbon film for biomedical applications, Adv. Mater. Sci. Eng. 11 (2019), https://doi.org/10.1155/2019/6812092. Article ID 6812092.
[30] L.A. Dobrzanski, M. Kremzer, A. Nagel, Aluminium EN AC-AlSi12 alloy matrix composite materials reinforced by Al_2O_3 porous preforms, Arch. Mater. Sci. Eng. 28 (10) (2007) 593–596, chromeextension://efaidnbmnnnibpcajpcglclefindmkaj/http://www.amse.acmsse.h2.pl/vol28_10/28104.pdf.
[31] Y.S. Katharria, S. Kumar, F. Singh, J.C. Pivin, D. Kanjilal, Synthesis of buried SiC using an energetic ion beam, J. Phys. D Appl. Phys. 39 (18) (2006) 3969–3973, https://doi.org/10.1088/0022-3727/39/18/007.
[32] J.A. Switzer, J. Hill, J.C. Mahenderkar, N. K., Y.C. Liu, Nanometer-thick gold on silicon as a proxy for single-crystal gold for the electrodeposition of epitaxial cuprous oxide thin films, ACS Appl. Mater. Interfaces 8 (24) (2016) 15828–15837, https://doi.org/10.1021/acsami.6b04552.
[33] Z. Abdullaeva, E. Omurzak, C. Iwamoto, H. Okudera, M. Koinuma, S. Takebe, S. Sulaimankulova, T. Mashimo, High temperature stable WC1−x@C and TiC@C core–shell nanoparticles by pulsed plasma in liquid, RSC Adv. 3 (2) (2012) 513–519, https://doi.org/10.1039/C2RA22028H.
[34] I. Pana, A. Constantin Vladescu, L.R. Sandu, I. G., M. Dinu, M.C. Cotrut, In vitro corrosion and tribocorrosion performance of biocompatible carbide coatings, Coatings 10 (7) (2020), https://doi.org/10.3390/coatings10070654, 654.
[35] J. Jiang, Y. Tzeng, Mechanisms of suppressing secondary nucleation for low-power and low-temperature microwave plasma self-bias-enhanced growth of diamond films in argon diluted methane, AIP Adv. 1 (4) (2011) 2158–3226, https://doi.org/10.1063/1.3656241.
[36] S. Pat, S. Temel, N. Ekem, S. Korkmaz, M. Özkan, M.Z. Balbağ, Diamond-like carbon coated on polyethylene terephthalate by thermionic vacuum arc, J. Plast. Film Sheeting. 27 (1–2) (2013) 127–137, https://doi.org/10.1177/8756087911399893.
[37] L. Ward, F. Junge, A. Lampka, M. Dobbertin, C. Mewes, M. Wienecke, The effect of bias voltage and gas pressure on the structure, adhesion and wear behavior of diamond like carbon (DLC) coatings with si ınterlayers, Coatings 4 (2014) 214–230, https://doi.org/10.3390/coatings4020214.
[38] B.A.J.W. Moore, W.J. McG, Relation between friction and hardness, Proc R Soc Lond A Math Phys Sci 212 (1952) 452–458, https://doi.org/10.1098/RSPA.1952.0234.
[39] J. Musil, M. Louda, Z. Soukup, M. Kubásek, Relationship between mechanical properties and coefficient of friction of sputtered a-C/Cu composite thin films, Diamond Relat. Mater. 17 (2008) 1905–1911, https://doi.org/10.1016/J.DIAMOND.2008.04.009.
[40] N.M. Mikhin, K.S. Lyapin, Hardness dependence of the coefficient of friction, Sov. Phys. J. 13 (1970) 317–332, https://doi.org/10.1007/BF00818317.
[41] P.J. Burnett, D.S. Rickerby, The relationship between hardness and scratch adhesion, Thin Solid Films 154 (1987) 403–416, https://doi.org/10.1016/0040-6090(87)90382-8.
[42] H. Cicek, I. Efeoglu, Fatigue and adhesion properties of martensite and austenite phases of TiNi shape memory thin films deposited by magnetron sputtering, Surf. Coat. Technol. 308 (2016) 174–181, https://doi.org/10.1016/j.surfcoat.2016.07.101.